Investigating the behaviour of PGEs during first-stage leaching of a Ni-Fe-Cu-S converter matte

by C.A. Snyders, G. Akdogan, G. Thompson, S.M. Bradshaw, and A.P. Van Wyk

Synopsis

In a first-stage atmospheric leach in a Sherritt Ni–Cu matte leach process, a Ni–Cu–Fe–S Peirce-Smith converter matte is contacted with recycled aqueous copper sulphate/sulphuric acid solution (spent solution) with the purpose of dissolving nickel, while simultaneously removing copper (via metathesis and cementation reactions) from solution. While the iron content has been found to have a significant impact on the first-stage leach, a previously expected relationship between copper and PGM behaviour has not been established clearly. For this study, a converter matte consisting mainly of heazlewoodite (Ni_3S_2), chalcocite (Cu_2S), and awaruite (Ni_3Fe) was leached in a laboratory-scale batch reactor. The temperature, acid, and copper concentration under both oxidative and non-oxidative conditions were varied, while the copper, iron, and PGEs were tracked and the pH and Eh measured. Palladium was generally found to be closely related to the behaviour of copper, while platinum did not leach. The other platinum group metals such as iridium and rhodium were found to precipitate only with accelerated precipitation being observed during Fe precipitation reactions.

Keywords
platinum group elements, converter matte, leaching.

Introduction

The primary goal of the Western Platinum Ltd base metal refinery (BMR) is to produce a high-grade platinum group element (PGE) concentrate with minimal losses to solution. According to Cole and Ferron (2002) the same processes, as used in the nickel and copper-nickel refineries (such as the Stillwater refinery), are being used for the PGE base metal refineries. There are mainly two commercial processes for the high-grade PGE refineries, the Outokumpu process (Hartley Platinum Zimbabwe, now closed) and the Sherritt Gordon process (Lonmin, Anglo Platinum, Impala Platinum, Noril'sk Nickel), each having the same underlying chemistry. A simplified block flow diagram of the Western Platinum Ltd (Lonmin) BMR is shown in Figure 1.

The atmospheric first-stage leach takes place in five continuous stirred tank reactors, which are connected in series. The first three reactors are operated under oxidative conditions while the remaining two operate under non-oxidative conditions. In order to recover PGEs that were leached during the

pressure leach, conditions that promote PGE precipitation in the first-stage (atmospheric) leach need to be established. The copper concentration is regarded as a leading indicator of PGE behaviour in plant operations, but this relationship has not been conclusively established (van Schalkwyk, Eksteen, and Akdogan, 2013). The results by van Schalkwyk, Eksteen, and Akdogan (2013) showed that the behaviour of copper in oxygenated tests may possibly be used as an indicator of whether PGE precipitation will take place, but during non-oxygenated tests, the copper precipitation was found to be a poor indicator.

Batch experiments similar to those by van Schalkwyk, Eksteen, and Akdogan (2013) were performed with the main aim of investigating the link between PGE and copper behaviour (Thompson, 2016). In these experiments, batch oxidative and non-oxidative leaches were performed in order to simplify the process to understand the chemistry separately. The more complex conditions of non-oxidation following oxidation in the same reactor (simulating plant conditions more closely), where the leaching, cementation and precipitation reactions will be intertwined and acid levels, pH, Eh, solid/liquid ratio and individual concentrations are unknown, are currently under investigation.

Materials and method

The batch leaching tests were carried out in the reactor set-up shown in Figure 2. The

---

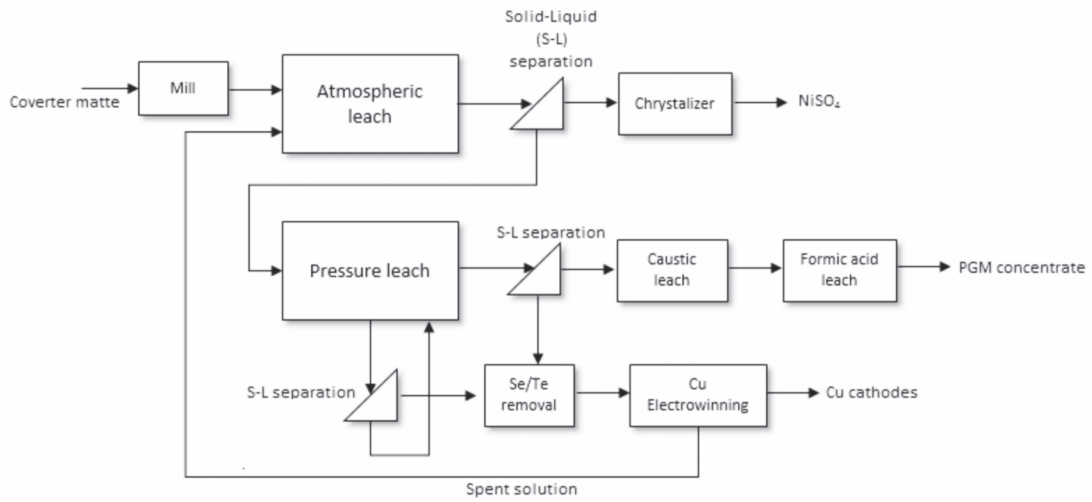* Stellenbosch University, Matieland, South Africa.

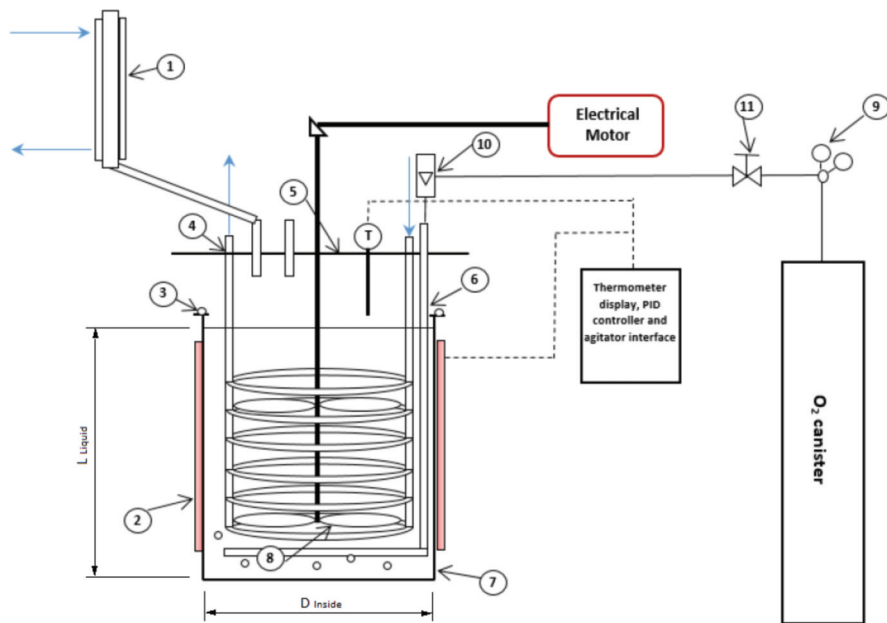**Figure 1—Flow diagram of the Lonmin base metal refinery**

Figure 2—Schematic and photo of the laboratory atmospheric batch leaching reactor

Investigating the behaviour of PGEs during first-stage leaching of Ni-Fe-Cu-S converter matte

Description of experimental equipment components

Label	Description
1	Liebig condenser to avoid unnecessary evaporation of reactor contents
2	Cylindrical electric heating jacket
3	Rubber O-ring seal to create a seal between reactor vessel and reactor lid
4	Cooling water coil to remove excess reactor heat due to leaching reactions
5	Thermometer as well as liquid sample port
6	Inlet oxygen dispersion device
7	Stainless steel reactor vessel
8	Agitation blades
9	Oxygen regulator
10	Oxygen flow meter (L/min)
11	Manual oxygen flow valve

Table III

Experimental design

Variable	Unit	Low	High
Copper	g/L	9.6	19.3
Acid	g/L	40	80
Temperature	°C	75	85
Oxygen	L/min	0	0.2

Table IV

Matte composition

Mineral phase	wt %
Heazlewoodite (Ni_3S_2)	58
Chalcocite (Cu_2S)	19.6
Magnetite (Fe_3O_4)	0.2
Tenorite (CuO)	0.4
Awaruite (Ni_3Fe_2)	21.8
Total	**100**

Table V

Spent solution composition

Species	Concentration
Ni^{2+} (g/L)	51.6
Cu^{2+} (g/L)	19.3
Co^{2+} (ppm)	322.5
Fe^{3+} (ppm)	295.1
Ir (ppm)	24.2
Pd (ppm)	3.0
Rh (ppm)	39.21
Ru (ppm)	213.7
Pt (ppm)	0.00
H_2SO_4 (g/L)	79.8

component descriptions are given in Table I and the reactor dimensions (scaled down from Lonmin atmospheric leach reactors, van Schalkwyk, 2011; van Schalkwyk *et al.*, 2011) given in Table II. The reactor was scaled down geometrically from the reactors used at Lonmin Marikana. A minimum diameter of 200 mm was chosen to eliminate wall effects and for the mixing to be similar to the process from which the reactor was scaled down from. The length of the reactor was subsequently chosen to obtain the same length/diameter ratio that applies to the plant reactors. The flow rate was obtained by scaling down by multiplying the plant flowrate with the laboratory reactor liquid volume to plant liquid volume ratio. The stirring rate was scaled in order to obtain equal solids suspension in the laboratory reactor.

Four litres of leach solution was heated to the required temperature (Table III) while being stirred at 1100 r/min at the required oxygen flow rate, which was blown in below the impeller. Once the reactor had reached the required temperature, the first liquid sample was taken. The temperature was maintained at the set-point throughout the tests by using a band heater and a programmable logic controller. The matte was then added to the solution in a solid/liquid ratio of 150 g/L and subsequent solution samples were taken at 15, 30, 60, 120, 150, and 180 minutes and filtered with a 0.45 μm syringe filter.

The leach tests were conducted by varying the initial copper, initial acid concentration, and temperature under oxidative and non-oxidative conditions as shown in Table III.

Table II

Comparisons of pilot plant and actual plant reactor

Dimension	Actual plant	Pilot plant
No. of baffles	4	4
l_{liquid} (mm)	2600	210
$d_{impeller}$ (mm)	1150	90
d_{inside} (mm)	2865	190
Reactor volume (m³)	16.7	6 (L)
Stirring rate (r/min)	88	1100

The composition of the matte was determined by XRD analysis and is shown in Table IV. The mineralogy of granulated Ni-Cu-S converter matte produced at Lonmin Marikana has been thoroughly described by Thyse *et al.*, (2010), Thyse *et al.*, (2013) and van Schalkwyk (2011). The same major phases were observed in the current work.

The spent solution (return anolyte from the copper electrowinning cells) was received from Lonmin and analysed with ICP-OES for base metals and PGMs. The concentrations are shown in Table V. The acid level was determined by precipitating out all the metals with a $Na_2CO_3/NaHCO_3$ buffer and analysing with high-performance liquid chromatography to determine the sulphate concentration. The spent solution was diluted by 50% volume and the copper concentration or the sulphuric acid was then increased by adding copper sulphate or sulphuric acid.
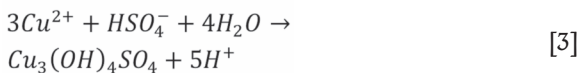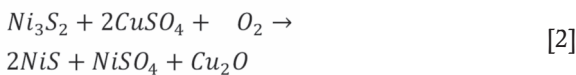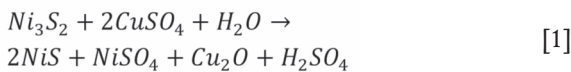
Sample analysis

For the pH and Eh measurements, a Eutech pH700, capable of taking pH and Eh readings at temperatures up to 100°C, was used. Liquid samples were analysed by atomic absorption spectrometry (AAS) for Cu and Fe and inductive couple plasma optical emission spectrometry (ICP-OES) for PGMs.

Investigating the behaviour of PGEs during first-stage leaching of Ni-Fe-Cu-S converter matte
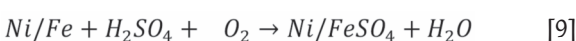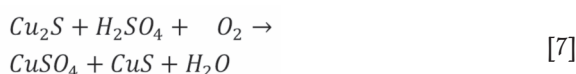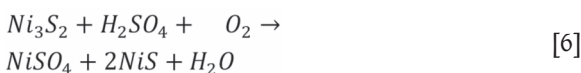
Results

Effect of oxygen

The effect of oxygen is shown in Figure 3, where it is indicated that a higher degree of precipitation for Ir, Rh, and Pd, as well as Cu, occurred under oxidative conditions. This is similar to the findings of van Schalkwyk, Eksteen, and Akdogan (2013) with regard to low-Fe mattes. Pt was found not to leach and subsequently did not precipitate either and was therefore not included in further results. The pH and Eh values with time for both the oxidative and non-oxidative tests are shown on the Pourbaix diagram in Figure 4. This clearly illustrates the difference between these two tests, with the oxidative tests ending in the Cu_2O stability zone where reactions are expected to take place according to Equation [1] (Symens *et al.*, 1979), Equation [2] (Llanos, Queneau, and Rickard, 1974), and probably Equation [3] (Hofirek and Kerfoot, 1992).

$$Ni_3S_2 + 2CuSO_4 + H_2O \rightarrow \\ 2NiS + NiSO_4 + Cu_2O + H_2SO_4 \qquad [1]$$

$$Ni_3S_2 + 2CuSO_4 + \ O_2 \rightarrow \\ 2NiS + NiSO_4 + Cu_2O \qquad [2]$$

$$3Cu^{2+} + HSO_4^- + 4H_2O \rightarrow \\ Cu_3(OH)_4SO_4 + 5H^+ \qquad [3]$$

For the non-oxidative conditions, Equation [4] is expected to be dominant. Some Cu alloy is expected to form due to the presence of 21.8% Ni-Fe alloy (awaruite, Table IV) as per Equation [5]. Van Schalkwyk (2011) also suggested that it is likely that iron will take part in the exchange reactions with copper, and stated that these would be similar to the cementation and metathesis reactions given for nickel.

$$Ni_3S_2 + 2Cu^{2+} \rightarrow Cu_2S + NiS + 2Ni^{2+} \qquad [4]$$

$$Ni^\circ + Cu^{2+} \rightarrow Cu^\circ + Ni^{2+} \qquad [5]$$
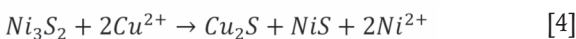
For the tests conducted under oxidative conditions, it was clear that there was a rapid consumption of acid with the solution pH increasing significantly to allow for iron hydrolysis to occur. The dominant acid-consuming reactions (Equations [6] to [9]) are expected to be (van Shalkwyk *et al.*, 2011):

$$Ni_3S_2 + H_2SO_4 + \ O_2 \rightarrow \\ NiSO_4 + 2NiS + H_2O \qquad [6]$$

$$Cu_2S + H_2SO_4 + \ O_2 \rightarrow \\ CuSO_4 + CuS + H_2O \qquad [7]$$

$$Cu + H_2SO_4 + {}^1\!/_2 O_2 \rightarrow CuSO_4 + H_2O \qquad [8]$$

$$Ni/Fe + H_2SO_4 + \ O_2 \rightarrow Ni/FeSO_4 + H_2O \qquad [9]$$

The ferrous iron will be oxidized to the ferric state, which will become unstable as the pH increases. Hydrolysis will follow as per Equations [10] and [11] (van Schalkwyk *et al.*, 2011; Hofirek and Kerfoot, 1992).

$$Fe^{3+} + 3H_2O \rightarrow Fe(OH)_3 + 3H^+ \qquad [10]$$

$$Fe^{3+} + HSO_4^- + H_2O \rightarrow Fe(OH)SO_4 + 2H^+ \qquad [11]$$
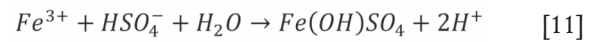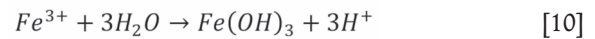
Both Ir and Rh precipitation were also found to accelerate with the iron hydrolysis reactions. This was not the case for Pd, which closely followed the precipitation of Cu. Van Schalkwyk, Eksteen, and Akdogan (2013) assumed that Rh, Ru, and Ir are cemented (Equation [12]) similarly to copper (Equation [5]), while Aktas (2011) proposed an almost identical cementation reaction for Rh onto Zn. Dorfling (2012) agreed that the precipitation of Rh, Ir, and Ru proceeds primarily via precipitation reactions similar to the cementation and metathesis reactions of copper precipitates, and in addition to Equation [12] proposed several more reactions that could potentially contribute to the precipitation behaviour of Rh, Ru, and Ir.

$$Ni^\circ + (Rh, Ir, Ru)SO_4 \rightarrow NiSO_4 + (Rh, Ir, Ru)^0 \qquad [12]$$

Milbourne, Tomlinson, and Gormely (2003) stated that hydrated ferric iron precipitates are reactive towards dissolved PGMs, but did not elaborate any further. The acceleration is, therefore, speculated to be due to one of the following two mechanisms. The first is a possible shift from homogenous nucleation (Equation [12]) to heterogeneous nucleation when $Fe(OH)_3$ and $Fe(OH)SO_4$ (such as shwertwannite or similar) start precipitating, leading to a physical agglomeration (for example $(Fe, Ir, Rh)(OH)_3$) of nanonuclei on the Fe surfaces. The second possible mechanism may be the formation of Ir or Rh hydroxy-sulphates $((Rh, Ir)(OH)_4SO_4)$ similarly to Equation [3] and Equation [11], which is associated with higher pH and Eh values. The stability diagrams for Ir and Rh (Figure 5 and 6), however, rather point to the formation of Ir and Rh (Equation 12), which effectively rules out the second suggested mechanism of Ir or Rh hydroxy-sulphates $((Rh, Ir) (OH)4SO4)$.

Effect of acid concentration

The most pronounced effect of the initial acid concentration was seen on the Fe and Cu behaviour as per Figure 7. For the higher initial acid concentration of 80 g/L, the Fe leaching rate was faster and, as expected, Fe precipitation/hydrolysis occurred at a much later stage.

Cu initially precipitated out of solution at approximately the same rate (Equations [1] to [5]) for both high and low acid concentrations, but was found to leach back into solution at the higher acid concentration (Equations [7] and [8]). Van Schalkwyk *et al.*, (2011) also found that copper leaching occurred only after the experiment had started, and attributed this to the possibility that the chalcocite was exposed to leaching only after a period of Ni leaching led to pore formation in the heazlewoodite matrix. The continued Cu precipitation in the low-acid run is likely due to the formation of antlerite (Equation [3]) as the acid was consumed and the pH increased to 4 (van Shalkwyk *et al.*, 2011; Hofirek and Kerfoot, 1992). Pd closely followed the behaviour of copper.
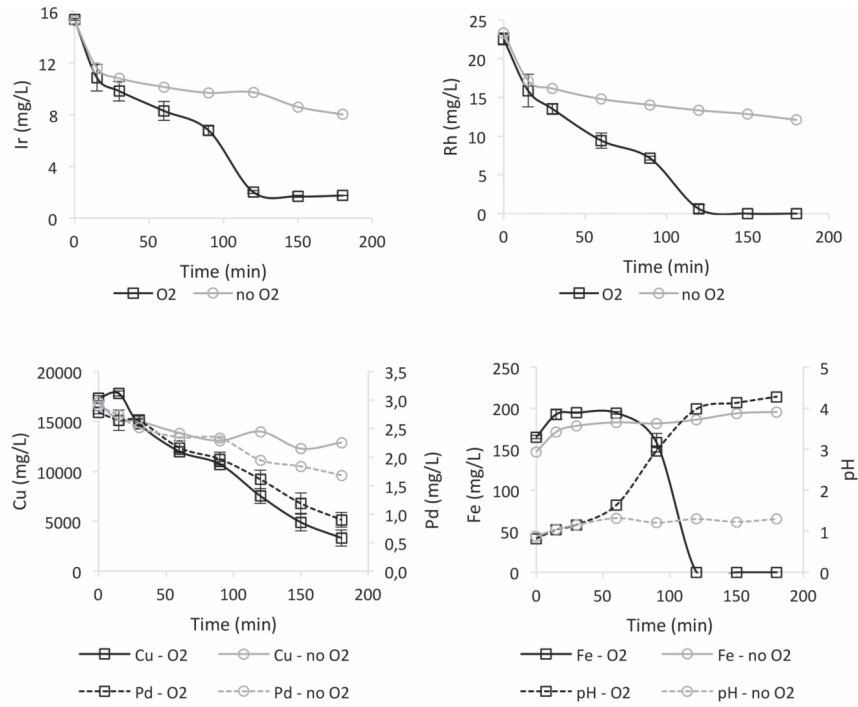
Figure 3—Extractions under oxidative and non-oxidative leaching tests, including standard error (Cu 19.3 g/L, initial acid 40 g/L, 75°C)
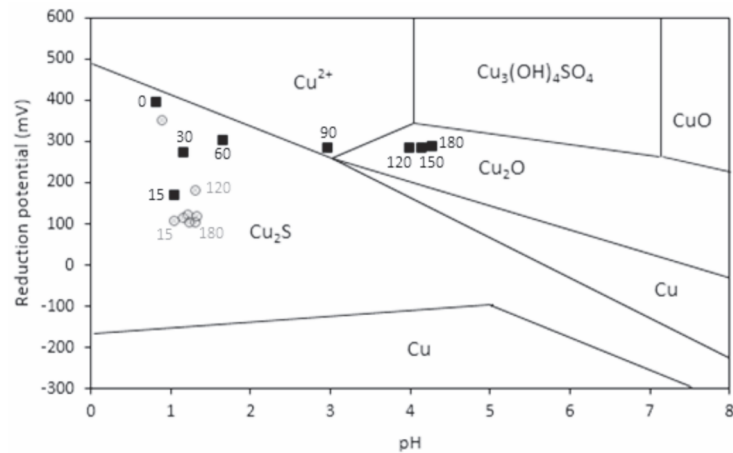
Figure 4—Stability diagram for Cu-Ni-S-H$_2$O system at 80°C (redrawn from Lamya, 2007), with the squares indicating the leaching tests (present study) with O$_2$ and the circles without O$_2$. The time in minutes is shown next to each measurement point
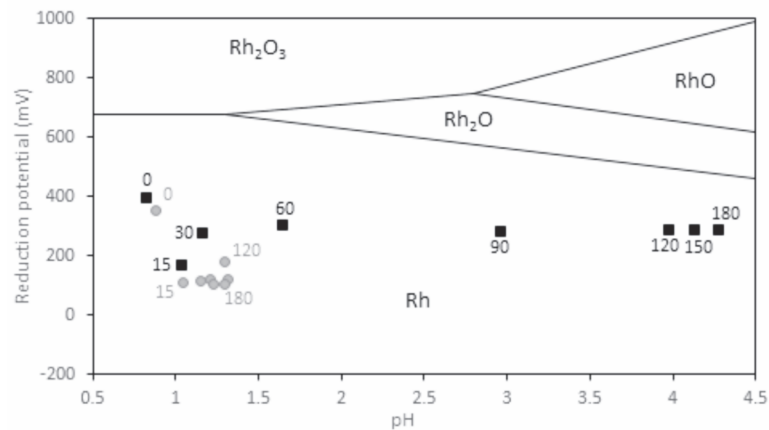
Figure 5—Stability diagram for Iridium for the atmospheric leach liquor at 90°C, 1bar (redrawn from Coetzee *et al.*, 2018), with the squares indicating the leaching tests (present study) with O$_2$ and the circles without O$_2$. The time in minutes is shown next to each measurement point
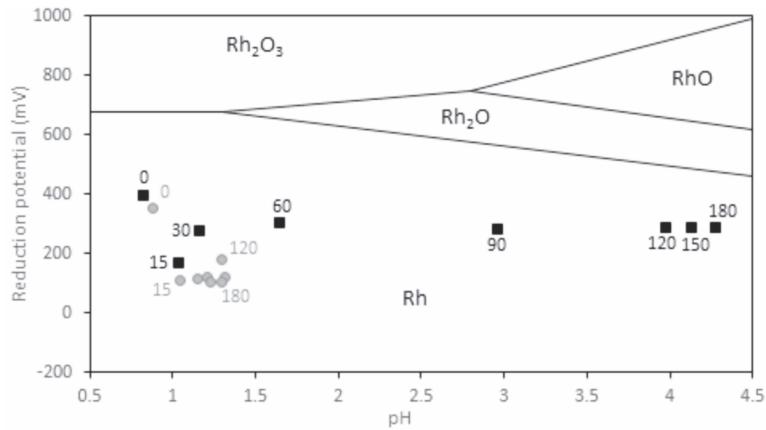
Figure 6—Stability diagram for rhodium for the atmospheric leach liquor at 90ºC, 1 bar (redrawn from Coetzee *et al.*, 2018) with the squares indicating the leaching tests (present study) with O_2 and the circles without O_2. The time in minutes is shown next to each measurement point
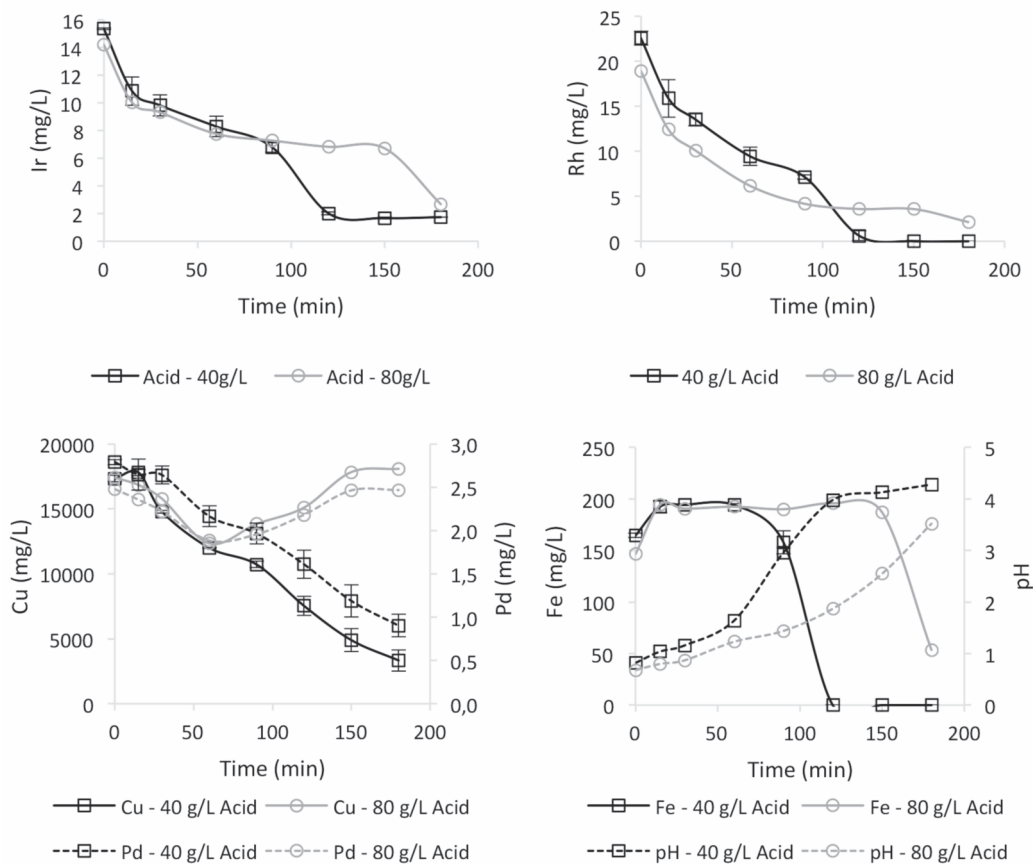

Figure 7—Extractions at 80 g/L and 40 g/L initial acid concentration including standard error (Cu 19.3 g/L, 75° C, O_2 0.2 L/min)

The Ir and Rh precipitation for both high and low acid concentrations was almost identical, with the only difference being the accelerated precipitation occurring in conjunction with the Fe hydrolysis reactions starting at approximately 90 minutes for the low initial acid concentration and at around 150 minutes for the higher initial acid concentration.

Effect of temperature

Increased operating temperature increased both the leaching rate and the precipitation rate (Figure 8). Similarly to a higher initial acid concentration, the Fe leaching rate increased with the higher temperature but the acid consumption and subsequent rise in pH was also faster at the higher temperature of 85ºC. This led to Fe hydrolysis occurring sooner, with Ir precipitation accelerating at this point again. In this case, the accelerated precipitation effect was less pronounced with Rh.

The Cu, Ir, and Rh precipitation rates were also observed to be faster at 85ºC than at 75ºC. This result agrees with Lamya (2007), who found that the cementation rate was drastically increased as the temperature was increased from 60ºC to 80ºC. It was concluded that the rate of cementation was controlled by a boundary layer diffusion mechanism at temperatures > 70ºC. Aktas (2011) also showed that Rh cementation reactions increased with temperature, similarly to Cu.
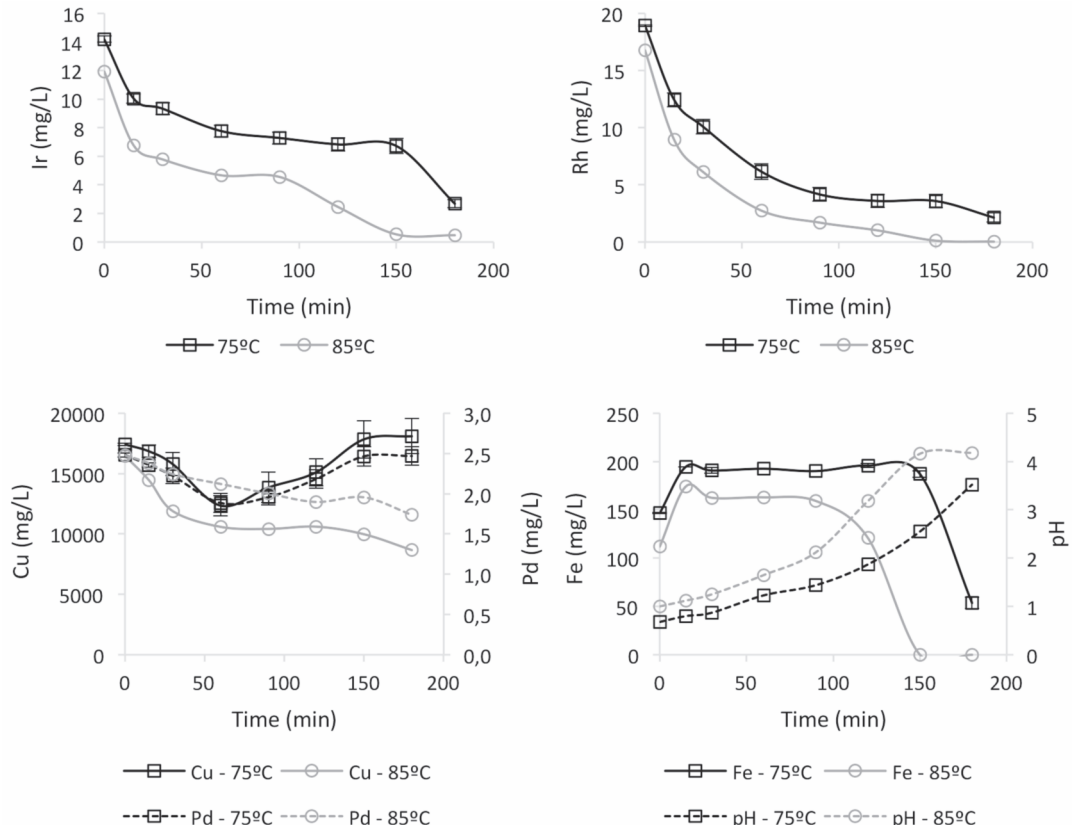
Figure 8—Extractions at 85ºC and 75ºC including standard error (Cu 19.3g/L, acid 80 g/L, O$_2$ 0.2 L/min).
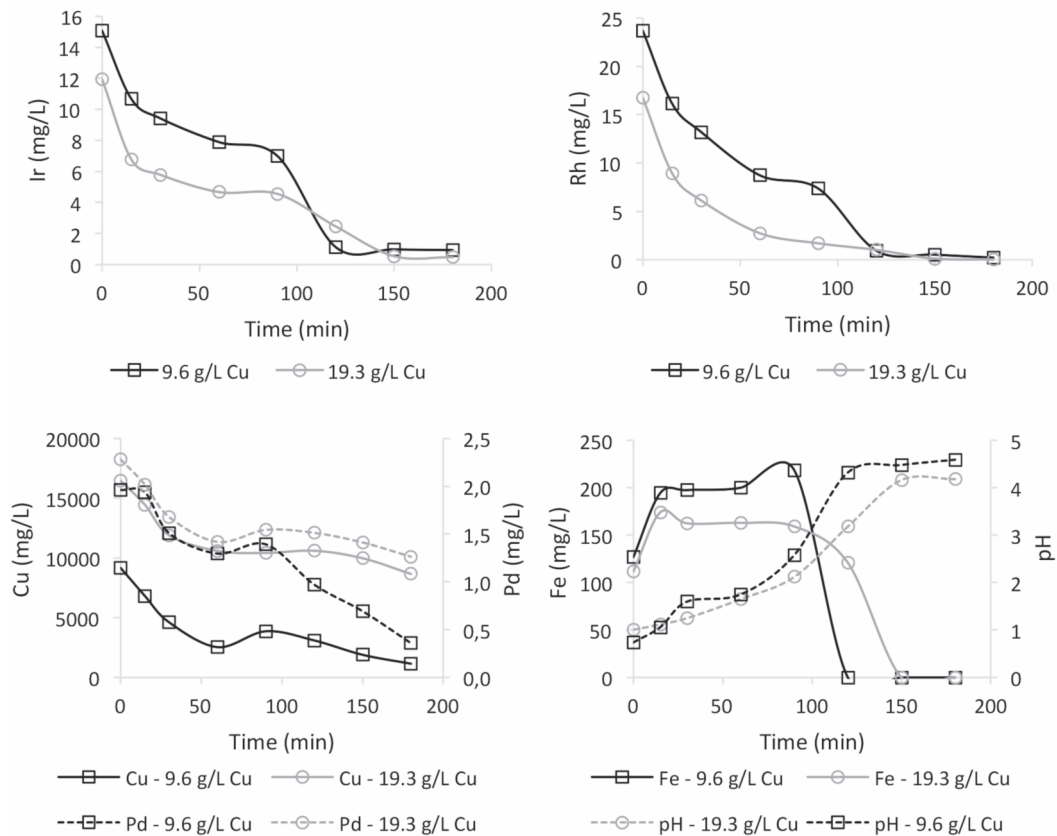
Figure 9—Extractions at 9.6 and 19.3 g/L Cu concentrations (acid 80 g/L, 85ºC, O$_2$ 0.2 L/min)

Investigating the behaviour of PGEs during first-stage leaching of Ni-Fe-Cu-S converter matte
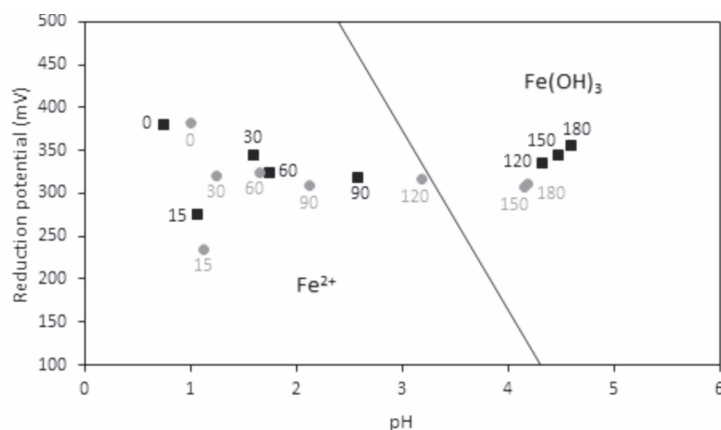

Figure 10. Stability diagram for the Fe-Cu-Ni-S-H_2O system at 80°C (redrawn from Lamya, 2007), with the squares indicating the present leaching tests at 9.6 g/L Cu and the circles at 19.3 g/L Cu. The time in minutes is shown next to each measurement point.

Effect of copper concentration

Slightly higher precipitation rates were seen for Ir and Rh with higher copper concentrations, as per Figure 9. Similarly to all previous cases, the Ir precipitation seems to be closely linked with the iron hydrolysis reactions, with a high rate of Ir precipitation when the Fe hydrolysis reactions are fast, as in the case of 9.6 g/L Cu concentration and slower acceleration as per the 19.3 g/L Cu concentration case. For Rh, this phenomenon was not as evident.

No specific effect of the Cu concentration could be seen on Fe leaching rates, which agrees with findings by van Schalkwyk (2011). Fe hydrolysis was rapid for both the low and high Cu concentrations at a pH of 3.2 (Figure 10), although some evidence of Fe precipitating at lower pH values (pH 2.1) can be seen in the case of 19.3 g/L Cu in Figure 9.

Conclusions

The relationship between Cu and PGE behaviour was investigated through a series of batch leach experiments simulating the first-stage atmospheric leach in the Lonmin base metal refinery. A low-Fe converter matte consisting mainly of heazlewoodite (Ni_3S_2), chalcocite (Cu_2S), and awaruite (Ni_3Fe) was leached in a laboratory-scale batch reactor while varying the temperature, acid and copper concentration under both oxidative and non-oxidative conditions.

In general, a higher degree of precipitation for Cu, Rh, and Ir under oxidative conditions for low-Fe mattes was found, which agrees with the findings by van Schalkwyk, Eksteen, and Akdogan (2013). More specifically, however, Ir and Rh precipitation were found to be independent of Cu behaviour, unlike Pd, which closely follows the precipitation and leaching behaviour of Cu. Accelerated precipitation for Ir and to a lesser extent for Rh, was observed in conjunction with iron hydrolysis reactions and was hypothesised to be due to hydrated ferric iron precipitates being reactive towards Rh and Ir, leading to a physical agglomeration (for example (Fe, Ir, Rh)$(OH)_3$) of nanonuclei on the Fe surfaces.

The acid concentration did not have an effect on Ir and Rh precipitation until the pH increased to the point where Fe started hydrolysing. An increase in temperature resulted in an increase in precipitation rate for Cu, Ir, and Rh, which agrees with findings by Lamya (2007) for Cu and Aktas (2011) for Rh cementation. Pt was found not to leach and subsequently did not precipitate either.

References

Aktas, S. 2011. Rhodium recovery from rhodium-containing waste rinsing water via cementation using zinc powder. *Hydrometallurgy*, vol. 106, pp. 71–75.

Dorfling, C. (2012). Characterisation and dynamic modelling of the behaviour of platinum group metals in high pressure sulphuric acid/oxygen leaching systems. PhD dissertation, University of Stellenbosch, South Africa.

Coetzee, R, Dorfling, and C, Bradshaw, S.M., 2018. Precipitation of Ru, Rh and Ir with iron ions from synthetic nickel sulphate leach solutions, *Hydrometallurgy*, Vol. 175, January 2018, pp. 79–92.

Cole, S. and Ferron, J., 2002. A review of the beneficiation and extractive metallurgy of the platinum group elements, Highlighting recent process innovations. SGS Mineral services, Technical paper 2002-03. http://www.sgs.com/-/media/global/documents/technical-documents/sgs-technical-papers/sgs-min-tp2002-03-beneficiation-and-extractive-metallurgy-of-pge.pdf

Hofirek, Z. and Kerfoot, D.G.E. 1992. The chemistry of the nickel-copper matte leach and its application to process control and optimisation. *Hydrometallurgy*, vol. 29, pp. 357–381.

Lamya, R.M. (2007). A fundamental evaluation of the atmospheric pre-leaching section of the nickel-copper matte treatment process. PhD dissertation, University of Stellenbosch, South Africa.

Llanos, Z.R., Queneau, P.B., and Rickard, R.S. 1974. Atmospheric leaching of matte at the Port Nickel Refinery. *CIM Bulletin*, vol. 67, pp. 74–81.

Milbourne, J., Tomlinson, M., and Gormely, L. (2003). Use of hydrometallurgy in direct processing of base metal/PGM concentrates. *Hydrometallurgy 2003 – Proceedings of the Fifth International Symposium*, Vancouver, Canada. Volume 1. Young, C.A., Alfantazi, A.M., Anderson, C.G., Dreisinger, D.B., Harris, B., and James, A. (eds). Wiley. pp. 617–630.

Symens, R.D., Queneau, P.B., Chou, E.C., and Clark, F.F. 1979. Leaching of iron containing copper-nickel matte at atmospheric pressure. *Canadian Metallurgical Quarterly*, vol. 18, pp. 145–153.

Thompson, G. 2016. Investigating the behaviour of Fe, Pt and Pd in the atmospheric sulphuric acid leaching of PGM containing Ni-Fe-Cu-S converter matte. Unpublished report, Department of Process Engineering, Stellenbosch University, November 2016.

Thyse, E., Akdogan, G., and Eksteen, J.J. 2010, The effect of changes in the iron-end-point during Peirce Smith converting on PGE-containing nickel converter matte mineralization, *Minerals Engineering*, Vol. 24, Issue 7, June 2011, pp. 688–697.

Thyse, E., Akdogan, G., Taskinen, P., Viljoen, K.S., and Eksteen, J.J., 2013. Towards understanding nickel converter matte solidification. *Minerals Engineering*, vol. 54, December 2013, pp. 39–51.

Van Schalkwyk, R.F. 2011. Leaching of Ni-Cu-Fe-S Peirce Smith converter matte: Effects of the Fe-endpoint and leaching conditions on the kinetics and mineralogy. MSc Eng. thesis, University of Stellenbosch, Stellenbosch.

Van Schalkwyk, R.F., Eksteen, J.J., and Akdogan, G. 2013. Leaching of Ni-Cu-Fe-S converter matte at varying iron endpoints; mineralogical changes and behaviour of Ir, Rh and Ru. *Hydrometallurgy*, vol. 136, pp. 36–45.

Van Schalkwyk, R.F., Eksteen, J.J., Petersen, J., Thyse, E.L., and Akdogan, G. 2011. An experimental evaluation of the leaching kinetics of PGM-containing Ni–Cu–Fe–S Peirce Smith converter matte, under atmospheric leach conditions. *Minerals Engineering*, vol. 24 no. 6, pp. 524–534. ◆